Arizona Press, Tucson, AZ, 1988), pp. 118–164.
4. B. Hapke, C. Christman, B. Rava, J. Mosher, *Proc. Lunar Planet. Sci. Conf.* **11**, 817 (1980).
5. B. Rava and B. Hapke, *Icarus* **71**, 397 (1987).
6. B. Hapke, G. E. Danielson, K. Klaasen, L. Wilson, *J. Geophys. Res.* **80**, 2431 (1975).
7. B. Hapke, *J. Atmos. Sci.* **33**, 1803 (1976).
8. M. J. Cintala, *J. Geophys. Res.* **97**, 947 (1992).
9. M. Benesh and M. Morrill, *Jet Propul. Lab. Doc. 615-148* (1973); G. E. Danielson, K. P. Klaasen, J. L. Anderson, *J. Geophys. Res.* **80**, 2357 (1975); J. M. Soha *et al.*, *ibid.*, p. 2394.
10. M. S. Robinson, B. R. Hawke, P. G. Lucey, *J. Geophys. Res.* **97**, 18265 (1992). The offset (signal inherent in the imaging system when no photons are impinging on the detector) was derived by averaging images acquired during the color sequence where Mercury did not appear in the frame—the camera was imaging nothing but deep space. As a test of the stability of the offset during the imaging sequence, the average offset image was subtracted from each frame of space acquired during the color sequence and no significant drift was measurable (camera A average residual was 0.3 DN; camera B average residual was 0.1 DN; possible range of DN 0–255). Examination of overlap between calibrated frames (dark corrected and linearized) revealed a maximum mismatch of 5%, with the average being 2%. Averaging areas of overlap between multiple frames reduced this residual in the final mosaics.
11. Applying Hapke modeling [B. W. Hapke, *Icarus* **67**, 264 (1986)] with parameters derived for the moon [P. Helfenstein and J. Veverka, *ibid.* **72**, 343 (1987); (*12*)] and those derived for Mercury resulted in overcorrection at the mercurian poles. Previous work with Galileo solid-state imager data has shown that Θ (theta bar) can be adjusted to compensate for such an overcorrection [A. S. McEwen and T. L. Becker, *Lunar Planet. Sci.* **XXIV**, 955 (1993)]. Iterative adjustment and visual inspection of the photometric flatness of the mercurian mosaic led us to use the following values for the Hapke parameters: $w = 0.21$, $h = 0.07$, $B_0 = 2.0$, $b = 0.29$, $c = 0.39$, and Θ (theta bar) = 15. It is known that the lunar photometric function varies subtly as a function of wavelength and composition (see McEwen and Becker, above), and the same is most likely true for Mercury. However, such minor effects will not hinder our identification of relative local color boundaries, which are key to the science presented here.
12. B. Hapke, *Phys. Earth Planet. Inter.* **15**, 264 (1977); J. Veverka, P. Helfenstein, B. Hapke, J. D. Goguen, in *Mercury*, F. Vilas, C. Chapman, M. S. Mathews, Eds. (Univ. of Arizona Press, Tucson, 1988) pp. 37–58.
13. F. Vilas, in *Mercury*, F. Vilas, C. Chapman, M. S. Mathews Eds. (Univ. of Arizona Press, Tucson, 1988) pp. 59–76.
14. T. B. McCord and J. B. Adams, *Icarus* **17**, 585 (1972); F. Vilas and T. B. McCord, *ibid.* **28**, 593 (1976); F. Vilas, M. A. Leake, W. W. Mendell, *ibid.* **59**, 60 (1984); F. Vilas, *ibid.* **64**, 133 (1985).
15. A. L. Sprague, R. W. H. Kozlowski, F. C. Witteborn, D. P. Cruikshank, D. H. Wooden, *ibid.* **109**, 156 (1994).
16. R. Jeanloz, D. L. Mitchell, A. L. Sprague, I. de Pater, *Science* **268**, 1455 (1995).
17. J. B. Adams, *J. Geophys. Res.* **79**, 4829 (1974).
18. P. G. Lucey, D. T. Blewett, J. L. Johnson, G. J. Taylor, B. R. Hawke, *Lunar Planet. Sci.* **XXVII**, 781 (1996).
19. B. Hapke, W. Cassidy, E. Wells, *Moon* **13**, 339 (1975); B. Hapke, in (*12*); R. V. Morris, *Proc. Lunar Planet. Sci. Conf.* **11**, 1697 (1980).
20. M. P. Charette, T. B. McCord, C. Pieters, J. B. Adams, *J. Geophys. Res.* **79**, 1605 (1974); E. Wells and B. Hapke, *Science* **195**, 977 (1977).
21. P. D. Spudis, *Proc. Lunar Planet. Sci. Conf.* **9**, 3379 (1978).
22. B. R. Hawke and J. W. Head, *ibid.*, p. 3285.
23. R. A. DeHon, D. H. Scott, J. R. Underwood, *U.S. Geol. Surv. Misc. Invest. Series Map I-1233* (1981).
24. T. Spohn, *Icarus* **90**, 222 (1991).
25. We find that the highest albedo materials in the mosaic (that is, crater Kuiper) are only about two times the global average (0.29 versus 0.14, respectively), whereas Hapke *et al.* (6) report the floor of Kuiper to be about three times the global average (0.45 versus 0.14). We are unable to explain the discrepancy satisfactorily and assume that it is due to improvements in our calibration.
26. We thank B. Hapke, G. J. Taylor, and B. R. Hawke for helpful reviews.

13 September 1996; accepted 6 December 1996

Activation of SAPK/JNK by TNF Receptor 1 Through a Noncytotoxic TRAF2-Dependent Pathway

Gioacchino Natoli,* Antonio Costanzo, Angelo Ianni, Dennis J. Templeton, James R. Woodgett, Clara Balsano, Massimo Levrero

Interaction of the p55 tumor necrosis factor receptor 1 (TNF-R1)–associated signal transducer TRADD with FADD signals apoptosis, whereas the TNF receptor–associated factor 2 protein (TRAF2) is required for activation of the nuclear transcription factor nuclear factor kappa B. TNF-induced activation of the stress-activated protein kinase (SAPK) was shown to occur through a noncytotoxic TRAF2-dependent pathway. TRAF2 was both sufficient and necessary for activation of SAPK by TNF-R1; conversely, expression of a dominant-negative FADD mutant, which blocks apoptosis, did not interfere with SAPK activation. Therefore, SAPK activation occurs through a pathway that is not required for TNF-R1–induced apoptosis.

Tumor necrosis factor is a pleiotropic cytokine that has growth modulatory, cytotoxic, and inflammatory activities (*1*). The effects of TNF are mediated by two distinct cell surface receptors of about 55 kD (TNF-R1) and 75 kD (TNF-R2), which are expressed on almost all nucleated cells (*2*). Proteins that are recruited to TNF-Rs after activation have been molecularly cloned, and their function has been partially characterized (*3*). The TNF-R1–associated death domain (TRADD) protein interacts with TNF-R1 upon TNF-induced trimerization, and its overexpression is sufficient to cause both activation of NFκB and apoptosis (*4*, *5*). Other proteins associated with TNF-R1 by way of TRADD include the death domain protein FADD (*5*, *6*) (which also participates in the transduction of Fas-induced apoptotic signals) and TRAF2 (*5*, *7*). TRAF2 belongs to a family of signal transducers for both the TNF-R superfamily and interleukin-1 receptor I (*8*). The TRAF family is characterized by a conserved COOH-terminal TRAF domain and, with the exception of TRAF1, an NH_2-terminal RING finger, which is relevant for signal transduction (*8*, *9*). An additional molecule required for TNF-R1 signal transduction is RIP, a death domain–containing protein kinase that participates in both activation of NFκB and promotion of apoptosis (*10*). Whereas FADD is required for TNF-R1–induced apoptosis, the interaction of TRADD with TRAF2 is required for activation of NFκB and is dispensable for cytotoxicity (*5*, *9*).

In addition to inducing apoptosis and activation of NFκB, cross-linking of TNF-R1 activates SAPK, also known as c-Jun NH_2-terminal kinase (JNK). SAPK binds to and phosphorylates the transcription factor c-Jun within its NH_2-terminal domain in cells exposed to environmental stresses [including TNF, ultraviolet (UV) light, protein synthesis inhibitors, and thermal stress] (*11*). The physiological consequences of SAPK activation have not been thoroughly defined. However, it has been shown that SAPK activity is required for apoptosis in nerve growth factor–deprived sympathetic neurons (*12*), as well as for stress-induced apoptosis in both leukemia cells and fibroblasts (*13*).

We therefore investigated the molecular mechanisms and the significance of TNF-induced activation of SAPK. Human embryonic kidney 293 cells contain very small amounts of endogenous TNF-R2, whereas TNF-R1 is constitutively expressed. Therefore, in these cells soluble TNF induces only TNF-R1 signaling (*5*, *9*). Treatment of 293 cells with human recombinant TNF-α (hrTNF-α) induces a rapid and transient in-

G. Natoli, A. Costanzo, A. Ianni, M. Levrero, Fondazione Andrea Cesalpino and Istituto di I Clinica Medica, Policlinico Umberto I, Viale del Policlinico 155, 00161 Rome, Italy.
D. J. Templeton, Case Western Reserve University School of Medicine, Biomedical Research Building, Cleveland, OH 44106, USA.
J. R. Woodgett, Ontario Cancer Institute–Princess Margaret Hospital, Toronto M5G 2M9, Canada.
C. Balsano, Dipartimento di Medicina Interna, Università di L'Aquila, L'Aquila, 67100, Italy.
*To whom correspondence should be addressed.

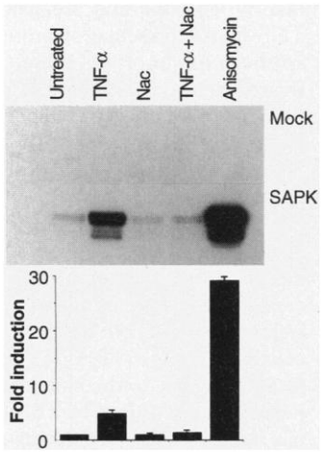

Fig. 1. TNF activation of SAPK in 293 cells. Cells plated on gelatin-coated 60-mm culture plates were transfected by calcium phosphate coprecipitation, with 4 μg of HA-p46SAPKγ-pCDNA3 (*14*). Forty-eight hours after transfection, cells that had first been treated or not with Nac (50 mM, 4 hours) were stimulated with hrTNF-α (2500 IU/ml) for 15 min. HA-SAPKγ was precipitated by detergent lysates with monoclonal antibody to HA (12CA5), and its activity was determined (*16*) with GST–c-Jun(1–141) as substrate. The fold induction over the basal activity was quantitated with a PhosphorImager. The results (mean ± SD) of two experiments are shown. Control experiments were performed with mock-transfected cells.

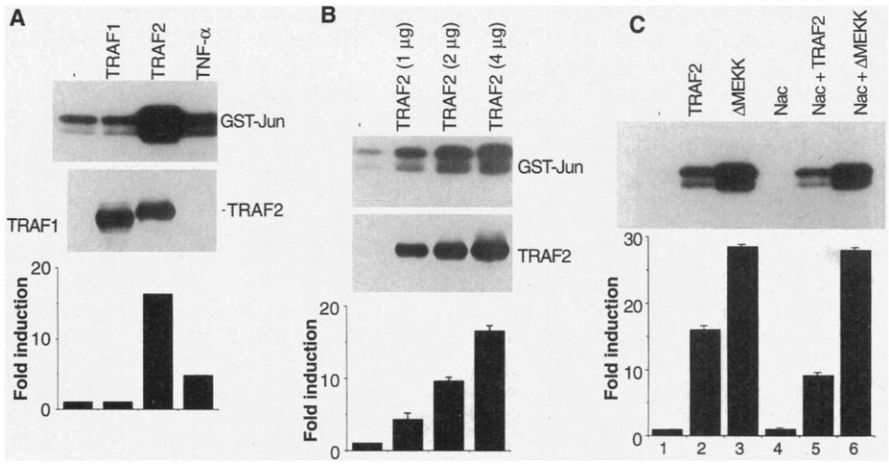

Fig. 2. Effects of TRAFs on SAPK activity in 293 cells. (**A**) TRAF2 activates SAPK. 293 cells were transfected with 4 μg of HA-p46SAPKγ-pCDNA3 (*14*) together with 4 μg of pRK-TRAF1 or pRK-TRAF2 (*9*). DNA concentration was always held constant by the addition of empty vector. Forty-eight hours after transfection detergent lysates were prepared, and the activity of exogenous transfected p46SAPKγ was determined (*14*). Expression of TRAF1 and TRAF2 in lysates from transfected cells is shown. Values shown are averages (mean ± SD) of four independent experiments. A Ser^{63,73}→Ala GST-Jun mutant was not phosphorylated by immunoprecipitated HA-SAPKγ (*19*). (**B**) Dose dependency of TRAF2-induced SAPK activation. The extent to which TRAF2 activated p46SAPKγ was dose dependent but did not further increase when amounts of pRK-TRAF2 greater than 4 μg per plate were used. (**C**) SAPK activation by TRAF2 is reduced by the anti-oxidant *N*-acetylcysteine. 293 cells were transiently cotransfected with 4 μg of HA-p46SAPKγ-pCDNA3 together with 4 μg of either pRK-TRAF2 (*9*) or pCMV-ΔMEKK (*18*). Forty-eight hours after transfection cells were treated with Nac (50 mM, 4 hours), and SAPK activity was determined (*14*). Nac had no effects on SAPK activation induced by either heat shock or osmotic stress (*19*), indicating that its inhibitory effect is selective for a subset of SAPK activators.

crease in SAPK activity that peaks at 15 min and reaches a maximal value of about three- to fivefold over the basal activity (Fig. 1) (*14*).

Reactive oxygen species (ROS) such as superoxide, hydrogen peroxide, and hydroxyl radical function as second messengers in TNF-induced signal transduction. In cells treated with TNF-α, ROS are produced rapidly and mediate both cytotoxicity (*15*) and NFκB activation (*16*). ROS are also implicated in SAPK activation by some stimuli, such as UV-C rays (*17*). Treatment of 293 cells with *N*-acetylcysteine (Nac), a thiol anti-oxidant and glutathione precursor, had no apparent effect on the basal SAPK activity. However, initial treatment with Nac is sufficient to block TNF-α–induced activation of SAPK (Fig. 1), suggesting that this activity of TNF is also dependent on ROS.

To examine a possible role for TRAFs in activation of SAPK, we cotransfected 293 cells with TRAF expression vectors together with a HA-p46SAPKγ-pCDNA3 plasmid (*14*). Forty-eight hours after transfection, HA-SAPKγ was recovered by immunoprecipitation with a monoclonal antibody to the HA epitope (clone 12CA5), and its activity was measured in an immune complex kinase assay with glutathione-S-transferase (GST)–c-Jun as a substrate (*14*). Expression of TRAF1 had no effect on SAPK activity; in contrast, expression of TRAF2 increased

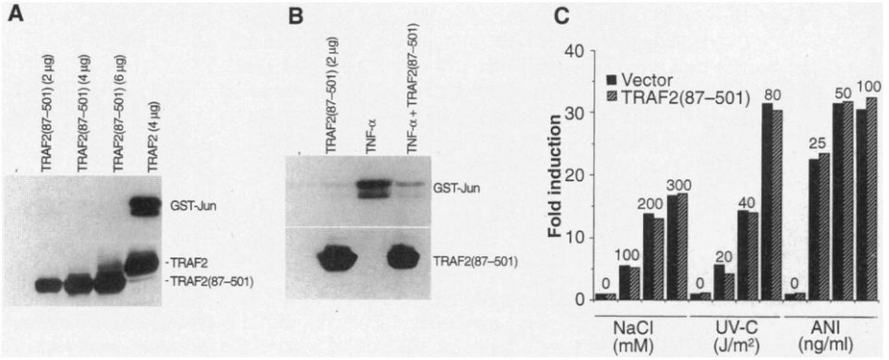

Fig. 3. A TRAF2 deletion mutant lacking the NH_2-terminal RING finger, TRAF2(87–501), acts as a dominant-negative inhibitor of TNF-induced SAPK activity. (**A**) The RING finger is required for SAPK activation by TRAF2. 293 cells transfected with various amounts of pRK-TRAF2(87–501) (*9*), and 4 μg of HAp46SAPKγ-pCDNA3 were analyzed for SAPK activity 48 hours after transfection as described (*14*). As a positive control, the effect of wild-type TRAF2 on SAPK activity is shown. 293 cell lysates from duplicate plates were subjected to protein immunoblot analysis with a rabbit polyclonal antibody raised against the COOH-terminus of TRAF2 (Santa Cruz). (**B**) TRAF2(87–501) blocks SAPK activation by TNF. HA-p46SAPKγ-pCDNA3 was cotransfected into 293 cells with either 4 μg of pRK-TRAF2(87–501) or vector. Forty-eight hours after transfection cells were stimulated with hrTNF-α (2500 UI/ml) for 15 min; detergent lysates were prepared and the activity of HA-SAPKγ was measured (*14*). Expression of TRAF2(87–501) in lysates from transfected cells is shown. (**C**) Effects of dominant-negative TRAF2 on SAPK induction by osmotic stress, UV-C, or anisomycin. 293 cells transfected with pRK-TRAF2(87–501) or vector plasmid were stimulated as indicated.

SAPK activity in a dose-dependent manner to a maximum of about 15-fold relative to the control (Fig. 2, A and B). The amount of SAPK activation obtained with TRAF2 is greater than that obtained with TNF-α (Fig. 2A), consistent with the presence of limiting amounts of endogenous TNFR1-TRADD-TRAF 2 complexes.

We next evaluated the effects of Nac on TRAF2-mediated activation of SAPK. Incubation with Nac (4 hours) reduced the extent to which SAPK was activated by

TRAF2 by about 40% (Fig. 2C). The induction of SAPK by MEK kinase (MEKK)—a protein kinase that phosphorylates and activates SEK, which in turn phosphorylates and activates SAPK (*18*)—is unaffected by Nac. This suggests that ROS are downstream of both TNF-R1 and TRAF2, but are upstream of MEKK. A longer incubation with Nac caused a greater inhibition of TRAF2-induced SAPK activity, but also caused some toxicity (*19*).

Activation of NFκB by TRAF2 requires the presence of the NH_2-terminal RING finger (*9*). In a similar manner, a TRAF2 mutant that lacks the first 86 amino acids, TRAF2(87–501) (*9*), had no effect on SAPK (Fig. 3A) even when expressed in large amounts. This TRAF2 mutant is still capable of both homotypic aggregation and interaction with TRADD; therefore, it acts as a dominant-negative inhibitor of both TNF-R1–, TNF-R2–, and TRADD-induced activation of NFκB (*5*, *9*). Overexpression of TRAF2(87–501) resulted in a complete suppression of TNF-induced SAPK activation (Fig. 3B), which indicates that TRAF2 is required for SAPK activation by TNF-R1. In contrast, osmotic stress–, UV-C–, and anisomycin-mediated activation of SAPK was not affected by TRAF2(87–501) (Fig. 3C).

We evaluated the role of FADD, a death domain–containing protein that acts as a transducer of both Fas- and TNF-R1–initiated apoptotic signals (*5*, *6*). FADD contains a COOH-terminal death domain, which mediates the association with the related death domains of Fas and TRADD (*5*, *6*), and an NH_2-terminal domain that is required for death induction and mediates the interaction with a downstream death effector known as MACH, FLICE, or Mch4 (*20*). A FADD mutant that lacks this NH_2-terminal effector domain, FADD(80–205), acts as a dominant-negative inhibitor of both TNF-R1–, TRADD-, and Fas-induced apoptosis (*5*, *6*). Overexpression of FADD(80–205) had no effect on basal SAPK activity. More importantly, it did not impair the ability of TNF to activate SAPK (Fig. 4), indicating that FADD is not a component of the TNF-R1–triggered signaling cascade resulting in SAPK activation.

We next studied the correlation between SAPK activation and TNF-induced apoptosis in HeLa cells. HeLa cells express predominantly TNF-R1 and are readily killed by TNF in the presence of protein- or RNA-synthesis inhibitors. In these cells, TNF activated SAPK about fourfold over basal activity; treatment with TNF plus actinomycin D (ActD) caused a similar activation of SAPK and induced cell death (Table 1). Activation of SAPK by either TNF or TNF plus ActD was completely blocked by TRAF2(87–501), the expression of which did not block apoptosis. In contrast, an increase in the number of apoptotic cells after treatment with TNF alone was observed in cells that express TRAF2(87–501); this effect may be due to the blockade of TNF-R1–induced activation of NFκB, which recently has been reported to protect against TNF-induced death (*21*). Thus, TNF-α–induced SAPK activation can be blocked at a membrane-proximal level without detrimental effects on cell death signaling. In a reciprocal manner, FADD(80–205) blocked apoptosis induced by TNF plus ActD but did not affect activation of SAPK (Table 1).

Our results confirm that induction of apoptosis by TNF-R1 requires FADD; however, FADD is not required for activation of SAPK by TNF-α, demonstrating that the TNF-α–induced apoptotic pathway is separate from the pathway that leads to SAPK activation. Conversely, TRAF2 is both necessary and sufficient for SAPK stimulation, and yet TRAF2 expression does not result in (and is not required for) cytotoxicity (Table 1).

The correlation of SAPK activation by TNF-α and TRAF2 with activation of NFκB suggests that SAPK may cause NFκB activation. Indeed, activation of SAPK by MEKK results in NFκB activation, and kinase-inactive MEKK blocks TNF-induced NFκB activation in some cellular models (*22*). However, in our system dominant-negative SEK did not block TRAF2-mediated SAPK activation (*19*), suggesting a possible divergence of the pathways leading to the activation of SAPK and NFκB downstream of TRAF2. TRAF2 is also a component of the signaling apparatus of CD40 (*9*), a TNF-R–related transmembrane receptor whose cross-linking triggers activation of both NFκB and SAPK (*9*, *23*). Because TRAF2 is required for CD40-induced NFκB activation (*9*), it may also mediate SAPK activation by this receptor.

Note added in proof: Liu *et al.* reported that recruitment of TRAF2 to the TNF-R1 complex mediates activation of SAPK/JNK (*24*).

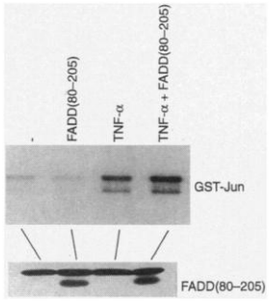

Fig. 4. Dominant-negative FADD does not interfere with SAPK activation by TNF. A FADD deletion mutant, FADD(80–205), that lacks the first 79 NH_2-terminal amino acids (*5*, *6*), which comprise the death effector domain (*5*, *6*), was expressed in 293 cells [4 μg of pRK-FADD(80–205)] together with HA-p46SAPKγ. Forty-eight hours after transfection cells were stimulated with TNF-α (2500 IU/ml, 15 min), and HA-SAPKγ activity was measured as above (*14*). Expression of Flag-tagged FADD(80–205) was analyzed by protein immunoblotting in lysates from transfected 293 cells with a rabbit polyclonal antibody to Flag (Santa Cruz). The upper band is nonspecific.

Table 1. Cell death and activation of SAPK by TNF and TNF-R1–associated proteins in HeLa cells. For apoptosis assays, HeLa cells were transiently transfected with a β-galactosidase expression vector (pCDNA HislacZ, 1 μg) in the presence or absence of 5 μg of the indicated expression constructs encoding TRAF1, TRAF2, TRAF2(87–501), or FADD(80–205), respectively (*5*, *9*). Forty-eight hours after transfection, the cells were treated with TNF in the presence or absence of ActD as indicated. After 12 hours the cells were fixed and stained with X-Gal. The data are expressed as the mean percentage (±SEM) of blue cells exhibiting signs of apoptosis (that is, intensely staining, shrunken blue cells showing loss of adherence) as a fraction of the total number of cells counted (shown in parentheses) (*25*). SAPK activation assays were performed as described (*14*). The data are from three independent experiments.

Expression vector	Treatment	Percent dead cells + SEM	SAPK activity
Vector	–	15.3 ± 1.2 (876)	1
Vector	TNF-α	14.6 ± 1.7 (830)	4.2 ± 0.5
Vector	ActD	24.5 ± 1.2 (780)	0.9 ± 0.2
Vector	TNF-α+ActD	96.2 ± 0.4 (143)	4.5 ± 0.8
TRAF1	–	13.8 ± 1.2 (910)	0.9 ± 0.3
TRAF2	–	12.7 ± 1.1 (935)	7.3 ± 1.2
TRAF2(87–501)	–	14.3 ± 1.3 (883)	1.3 ± 0.2
TRAF2(87–501)	TNF-α	41.0 ± 0.8 (462)	1.2 ± 0.4
TRAF2(87–501)	TNF-α+ActD	95.1 ± 0.3 (162)	1.1 ± 0.4
FADD(80–205)	–	13.7 ± 1.2 (897)	1.2 ± 0.2
FADD(80–205)	TNF-α	14.2 ± 1.1 (923)	4.5 ± 0.4
FADD(80–205)	TNF-α+ActD	18.3 ± 0.9 (753)	4.3 ± 0.5

REFERENCES AND NOTES

1. W. Fiers, *FEBS Lett.* **285**, 199 (1991); B. Beutler and A. Cerami, *Annu. Rev. Biochem.* **57**, 505 (1988).
2. L. A. Tartaglia and D. V. Goeddel, *Immunol. Today* **13**, 151 (1992); P. Vandenabeele, W. Declerq, R. Beyaert, W. Fiers, *Trends Cell Biol.* **5**, 392 (1995).

3. S. J. Baker and E. P. Reddy, *Oncogene* **12**, 1 (1996); M. Tewary and V. M. Dixit, *Curr. Opin. Genet. Dev.* **6**, 39 (1996).
4. H. Hsu, J. Xiong, D. V. Goeddel, *Cell* **81**, 495 (1995).
5. H. Hsu, H. B. Shu, M. G. Pan, D. V. Goeddel, *ibid.* **84**, 299 (1996).
6. M. P. Boldin *et al.*, *J. Biol. Chem.* **270**, 7795 (1995); A. M. Chinnaiyan, K. O'Rourke, M. Tewari, V. M. Dixit, *Cell* **81**, 505 (1995); A. M. Chinnaiyan *et al.*, *J. Biol. Chem.* **271**, 4961 (1996).
7. M. Rothe, S. C. Wong, W. J. Henzel, D. V. Goeddel, *Cell* **78**, 681 (1994).
8. H. M. Hu, K. O'Rourke, M. S. Boguski, V. M. Dixit, *J. Biol. Chem.* **269**, 30069 (1994); G. Mosialos *et al.*, *Cell* **80**, 389 (1995); T. Sato, S. Irie, J. C. Reed, *FEBS Lett.* **358**, 113 (1995); G. Cheng *et al*, *Science* **267**, 1494 (1995); C. H. Regnier *et al.*, *J. Biol. Chem.* **270**, 25715 (1995); H. Nakano *et al.*, *ibid.* **271**, 14661 (1996); Z. Cao, J. Xiong, M. Takeuchi, T. Kurama, D. V. Goeddel, *Nature* **383**, 443 (1996).
9. M. Rothe, V. Sarma, V. M. Dixit, D. V. Goeddel, *Science* **269**, 1424 (1995).
10. B. Z. Stanger, P. Leder, T. H. Lee, E. Kim, B. Seed, *Cell* **81**, 513 (1995); H. Hsu, J. Huang, H. B. Shi, V. Baichwal, D. V. Goeddel, *Immunity* **4**, 387 (1996).
11. V. Adler, A. Polotskaya, F. Wagner, A. S . Kraft, *J. Biol. Chem.* **267**, 17001 (1992); M. Hibi, A. Lin, T. Smeal, A. Minden, M. Karin, *Genes Dev.* **7**, 2135 (1993); J. M. Kyriakis *et al.*, *Nature* **369**, 156 (1994); B. Derijard *et al.*, *Cell* **76**, 1025 (1994).
12. Z. Xia, M. Dickens, J. Raingeaud, R. J. Davis, M. E. Greenberg, *Science* **270**, 1326 (1995); S. Estus *et al.*, *J. Cell Biol.* **127**, 1717 (1994); J. Ham *et al.*, *Neuron* **14**, 927 (1995).
13. M. Verheji *et al.*, *Nature* **380**, 75 (1996); B. W. Zanke *et al.*, *Curr. Biol.* **6**, 606 (1996).
14. HA-p46SAPKγ-pCDNA3 is a cytomegalovirus (CMV) promoter–based expression vector encoding a hemagglutinin (HA)–tagged version of a 46-kD splice variant of SAPKγ (*11*). TRAF expression vectors have been described (*5*, *9*). 293 cells were transfected by calcium phosphate coprecipitation with 8 μg of plasmid DNA. Forty-eight hours after transfection, cells were lysed in RIPA buffer containing 0.5 mM dithiothreitol (DTT), 20 mM β-glycerophosphate, 1 mM sodium orthovanadate, 10 mM sodium fluoride, 1 mM phenylmethylsulfonyl fluoride, leupeptin (20 μg/ml), and aprotinin (20 μg/ml). Lysates were cleared by centrifugation, and protein concentration was measured by use of a commercial Bradford protein assay (Promega). Equal amounts of each lysate (usually 500 μg) were incubated on ice with 2 μg of antibody to HA (12CA5, Boehringer) for 2 hours. Immune complexes were collected by protein A–agarose for 25 min, washed three times with RIPA buffer containing 20 mM β-glycerophosphate, 1 mM sodium orthovanadate, and 0.5 mM DTT, and then washed once with kinase reaction buffer (KRB) [20 mM Hepes (pH 7.5), 20 mM $MgCl_2$, 20 mM β-glycerophosphate, 2 mM DTT, 100 μM sodium orthovanadate, 0.5 mM sodium fluoride]. Samples were finally resuspended with 40 μl of KRB containing 20 μM adenosine 5′-triphosphate (ATP), 2.5 μCi of [γ-^{32}P]ATP, and 2 μg of GST–c-Jun(1–141) and incubated at 30°C for 20 min. Reactions were stopped by addition of 3× Laemmli sample buffer; samples were boiled and loaded on 12.5% SDS-polyacrylamide gels. After fixing and drying, gels were autoradiographed at −70°C. Radioactivity was quantitated with a PhosphorImager. The amount of HA-SAPKγ in each sample was analyzed by protein immunoblot on immunoprecipitates of 150-μg samples. Only experiments with comparable amounts of HA-SAPKγ in each sample were taken into consideration.
15. N. Yamauchi *et al.*, *Cancer Res.* **49**, 1671 (1989); R. J. Zimmermann, A. Chan, S. A. Leadon, *ibid.*, p. 1644; K. Schulze-Osthoff *et al.*, *J. Biol. Chem.* **267**, 5317 (1992); K. Schulze-Osthoff, R. Baeyaert, V. Vandevoorde, G. Haegerman, W. Fiers, *EMBO J.* **12**, 3095 (1993); V. Goossens, J. Grooten, K. DeVos, W. Fiers, *Proc. Natl. Acad. Sci. U.S.A.* **92**, 8115 (1995); P. Mehlen, C. Kretz-Remy, X. Preville, A. P. Arrigo, *EMBO J.* **15**, 2695 (1996).
16. R. Schreck, P. Rieber, P. A. Bauerle, *EMBO J.* **10**, 2247 (1991).
17. V. Adler, A. Schaffer, J. Kim, L. Dolan, Z. Ronai, *J. Biol. Chem.* **270**, 26071 (1995).
18. M. Yan *et al.*, *Nature* **372**, 798 (1994); I. Sanchez *et al.*, *ibid.*, p. 794.
19. G. Natoli *et al.*, unpublished results.
20. M. Muzio *et al.*, *Cell* **85**, 817 (1996); M. P. Boldin, T. M. Goncharov, Y. V. Goltsev, D. Wallach, *ibid.*, p. 803; T. Fernandes-Alnemri *et al.*, *Proc. Natl. Acad. Sci. U.S.A.* **93**, 7464 (1996).
21. A. A. Beg and D. Baltimore, *Science* **274**, 782 (1996); C.-Y. Wang, M. W. Mayo, A. S. Baldwin Jr., *ibid.*, p. 784; D. J. Van Antwerp, S. J. Martin, T. Kafri, D. R. Green, I. M. Verma, *ibid.*, p. 787.
22. M. Hirano *et al.*, *J. Biol. Chem.* **271**, 13234 (1996); C. F. Meyer, X. Wang, C. Chang, D. J. Templeton, T. H. Tan, *ibid*, p. 8971.
23. I. Berberich *et al.*, *EMBO J.* **14**, 5338 (1996).
24. Z. G. Liu *et al.*, *Cell* **87**, 565 (1996).
25. The β-galactosidase expression vector pCDNA-HislacZ is from Invitrogen. HeLa cells (2.5×10^5 per plate) were seeded on a 35-mm plate. Three hours later cells were transfected by calcium phosphate coprecipitation with 6 μg of total plasmid DNA. Forty-eight hours after transfection, the cells were treated with hrTNF-α (1000 IU/ml, Genzyme) with or without ActD (50 ng/ml). After 12 hours the cells were fixed in 3% formaldheyde-buffered saline and stained overnight with phosphate-buffered saline containing X-Gal (0.4 mg/ml), 4 mM potassium ferricyanide, 4 mM potassium ferrocyanide, and 4 mM $MgCl_2$. Blue cells were visualized by phase contrast microscopy; round blue cells showing intense blue staining and loss of adherence were considered as apoptotic. Results are expressed as the percentage of apoptotic blue cells among the total number of blue cells counted.

26. We thank D. V. Goeddel (Tularik, South San Francisco) for mTRAF1-pRK, mTRAF2-pRK, mTRAF2(87–501)-pRK, mFADD(80–205)-pRK, and mTRADD-pRK and for critically reading the manuscript. M. Karin is gratefully acknowledged for providing GST-Jun(1–223) ($Ser^{63,73}$→Ala). Supported by the Associazione Italiana Ricerca sul Cancro (AIRC), by the Consiglio Nazionale delle Ricerche (ACRO Project), and by Fondazione Andrea Cesalpino.

29 August 1996; accepted 26 November 1996

Regulation of Cell Cycle Synchronization by *decapentaplegic* During *Drosophila* Eye Development

Andrea Penton, Scott B. Selleck, F. Michael Hoffmann*

In the developing *Drosophila* eye, differentiation is coordinated with synchronized progression through the cell cycle. Signaling mediated by the transforming growth factor–β–related gene *decapentaplegic* (*dpp*) was required for the synchronization of the cell cycle but not for cell fate specification. DPP may affect cell cycle synchronization by promoting cell cycle progression through the G_2-M phases. This synchronization is critical for the precise assembly of the eye.

The *Drosophila* eye has served as a model system for examining the molecular mechanisms that govern the patterning and assembly of a complex tissue. The adult eye develops from an epithelial monolayer known as the eye imaginal disc. Differentiation begins in the posterior end of the disc and progresses anteriorly, marked by an indentation in the disc epithelium called the morphogenetic furrow (MF). Within the MF, unpatterned cells are induced to differentiate into the highly ordered array of retinal cells and nonneural accessory cells that produce the 750 ommatidia of the adult eye (*1*, *2*). Differentiated cells posterior to the MF express the signaling molecule hedgehog (HH), which directs the anterior advancement of the furrow (*3*, *4*) and induces the expression of DPP within the furrow. DPP mediates cell fate determination in the developing wing and leg in response to HH (*5*, *6*).

During the initial stages of sensory unit assembly in the MF, precursor cells exhibit synchronization of the cell division cycle (*2*, *7*). Anterior to the MF, cells divide randomly, but just ahead and within the MF, cell divisions occur more coordinately. The first evidence of cell cycle synchronization is increased amounts of cyclin B (*8*), a mitotic cyclin required for entry into mitosis (*9*). As cells enter late G_2, cyclin B levels peak and cyclin B then degrades at the metaphase-anaphase transition in mitosis. Loss of cyclin B and the appearance of mitotic figures mark coordination in the M phase (Fig. 1, A through C). After completion of mitosis, cells arrest in G_1 in the MF and transcription of *dpp* is activated (Fig. 1C).

Cells respond to DPP through two type I receptors, *thick veins* (*tkv*) or *saxophone* (*sax*), and a type II receptor, *punt* (*put*) (*10*). Responses to DPP are also attenuated by mutations in the putative transcription factor *schnurri* (*shn*) (*11*). We examined whether DPP was necessary for cell fate specification or cell cycle synchronization by determining whether cells defective for *tkv*, *sax*, or *shn* showed abnormalities in cell division or dif-

A. Penton and F. M. Hoffmann, McArdle Laboratory for Cancer Research and Laboratory of Genetics, University of Wisconsin Medical School, Madison, WI 53706, USA. S. B. Selleck, Arizona Research Laboratories Division of Neurobiology and Department of Molecular and Cellular Biology, University of Arizona, Tucson, AZ 85721, USA.

*To whom correspondence should be addressed.